

# On Motion Coordination of Multiple Vehicles with Nonholonomic Constraints

Feng Xie and Rafael Fierro

**Abstract**—Coordination of multiple vehicles has been of great interest in the control community. In this paper, we consider the problem of controlling a team of mobile robots with nonholonomic constraints to leader-following formations. We propose that it is more convenient to put the nonholonomic constraints inside the model predictive control (MPC) framework. As the first step of exploration, a dual-mode MPC algorithm is developed. The stability of the formation is guaranteed by constraining the terminal state to a terminal region and switching to a stabilizing terminal controller at the boundary of the terminal region. The effectiveness of the method is investigated by numerical simulations.

## I. INTRODUCTION

Teams of mobile robots operating cooperatively lead to many advantages, such as cost-effectiveness, fault tolerance and robustness. One interesting problem in multi-robot coordination is how to drive a group of robots to a desired formation. Unmanned ground vehicle (UGV) formations can provide a promising and efficient alternative to existing techniques in a wide range of applications. The most appealing one is the envisioned distributed sensing tasks. Many researchers have been working on formation problems, and numerous control algorithms can be found in the literature (see *e.g.*, [1], [2], [3]).

A nonholonomic model (*e.g.*, unicycle) is commonly adopted to describe vehicle's kinematics in UGV coordination. Basic problems, such as trajectory tracking, point stabilization and path following, have been studied for many years. According to Brockett [4], a smooth time-invariant feedback control law doesn't exist for the point stabilization problem. Discontinuous time-invariant or time-variant algorithms have been proposed (see *e.g.* [5], [6]). Only a few controllers which can handle the tracking and stabilization problems in the same control structure are found in the literature [7].

Recently, model predictive control (MPC) or receding horizon control (RHC) has gained more and more attention in the control community. The inherent ability of MPC to handle constrained systems makes it a promising technique for cooperative control, especially for multi-vehicle formation control. Recent work includes [2], [3]. The stability and feasibility of the MPC algorithms become a new challenge (see discussion in [8]). MPC details and its properties can be found in [9]. Applications of MPC controlling nonholonomic mobile robots are described in [10], [11].

F. Xie and R. Fierro are with the MARHES Lab, School of Electrical and Computer Engineering, Oklahoma State University, Stillwater, OK 74078, USA {feng.xie, rfierro}@okstate.edu

In this paper, based on previous work [12], [13], we show that it is more convenient to put the vehicles's nonholonomic constraints inside the MPC framework. Moreover, we present a novel MPC algorithm for mobile robot formations. Since a stabilizing terminal controller is switched in within a specified terminal constraint set, the proposed MPC algorithm is dual-mode [14]. With this dual-mode MPC implementation, stability is achieved while feasibility is relaxed. For the choice of stabilizing terminal controller, a comparison between an input-output feedback linearization controller used in [12] and a robust formation controller used in [13] is given.

The rest of the paper is organized as follows. In Section II, some preliminaries are briefly introduced. A dual-mode MPC algorithm are proposed in Section III. Stability results are provided in Section IV. Section V contains simulation results. Finally, concluding remarks and future work are given in Section VI.

## II. PRELIMINARIES

The problem considered in this paper is to drive a team of nonholonomic vehicles to a desired formation. This section describes the model used for the mobile agents and the definition of formation.

### A. Vehicle Model

Consider the planar motion of nonholonomic unicycle-model robots whose kinematics are determined by

$$\begin{bmatrix} \dot{x}_i \\ \dot{y}_i \\ \dot{\theta}_i \end{bmatrix} = \begin{bmatrix} \cos \theta_i & 0 \\ \sin \theta_i & 0 \\ 0 & 1 \end{bmatrix} \begin{bmatrix} v_i \\ \omega_i \end{bmatrix} \quad (1)$$

where the subscript  $i \in [1, \dots, N]$  indicates the  $i^{\text{th}}$  UGV.  $(x_i, y_i)$  are the Cartesian coordinates of the robot,  $\theta_i \in (-\pi, \pi]$  represents the orientation of the robot with respect to the positive  $x$  axis, and  $v_i$  and  $\omega_i$  are linear and angular velocities, respectively.

### B. Formation and Formation Control Graph

**Definition 2.1:** A formation is a network of agents interconnected via their controller specifications that dictate the relationships each agent must maintain with respect to its neighbors. The interconnections between agents are modeled as edges in a directed acyclic graph, labeled by a given relationship [15], [16].

**Definition 2.2:** A formation control graph  $\mathcal{G} = (\mathcal{V}, \mathcal{E}, \mathcal{F})$  is a directed acyclic graph consisting of the following:

- A finite set  $\mathcal{V} = (V_1, \dots, V_N)$  of  $N$  vertices and a map assigning each vertex  $V_i$  to a control system (1).

- An edge set  $\mathcal{E} \subset \mathcal{V} \times \mathcal{V}$  of pair-wise neighbors encoding the formation between agents. If the ordered pair  $(V_i, V_j) \in \mathcal{E}$ , then  $(V_j, V_i) \notin \mathcal{E}$ , and  $(V_k, V_j) \notin \mathcal{E}$  for all  $k \in \{1, \dots, N\} \setminus i$ .
- A set of constants  $\mathcal{F} = \{F_{ij}^d \in \mathbb{R}_- \times \mathbb{R}\}$  defining control objectives, or *set points*, for each node  $j$ , such that  $(V_i, V_j) \in \mathcal{E}$  for some  $V_i, V_j \in \mathcal{V}$ .

Consequently, by changing  $F_{ij}^d$ , we are able to define different formation shapes for the mobile robot team.

### III. CONTROLLERS FOR MULTI-ROBOT COORDINATION

Considering an operator specified the  $j^{\text{th}}$  robot motion  $a_i(t) \in \mathbb{R}^2$ ,  $i \in \{1, \dots, N\}$  is given as follows

$$a_i(t) = x_i(t)\hat{i} + y_i(t)\hat{j}, \quad (2)$$

where  $x_i(t)$  and  $y_i(t)$  represent the respective Cartesian coordinates in an earth-fixed reference inertial frame  $\mathcal{I}$ . Let  $F_{ij}^d = [\Delta x_{ij}^d \quad \Delta y_{ij}^d]^T$  be the desired formation between robots  $i$  and  $j$ .  $\Delta x_{ij}^d \in \mathbb{R}_-$  and  $\Delta y_{ij}^d \in \mathbb{R}$  are the desired position for robot  $j$  in a local Cartesian reference frame  $\mathcal{C}$  attached to robot  $i$ . Then the actual formation for robot-pair  $i$  and  $j$  is described by  $F_{ij} = [\Delta x_{ij} \quad \Delta y_{ij}]^T$ .

Usually, a robot can obtain its neighbors' positions by communication, sensing or both. When robots are close to each other, relative positions can be measured by onboard instruments and expressed in Polar coordinates. Let  $\bar{F}_{ij}^d = [l_{ij}^d \quad \eta_{ij}^d]^T$  be the desired formation between robots  $i$  and  $j$  in a frame attached to robot  $i$ , where  $l_{ij}^d \in \mathbb{R}_+$  is the desired distance and  $\eta_{ij}^d \in [\frac{\pi}{2}, \frac{3\pi}{2}]$  is the desired relative bearing angle. The actual formation for robot-pair  $i$  and  $j$  is described by  $\bar{F}_{ij}(t) = [l_{ij} \quad \eta_{ij}]^T$ , in which the relative distance is defined as  $l_{ij}(t) = \|a_i - a_j\|_2$ , where  $\|\cdot\|_2$  denotes the standard Euclidean norm. The relative bearing is given by  $\eta_{ij}(t) = \pi + \zeta - \theta_i$ , where  $\zeta(t) = \arctan 2(y_i - y_j, x_i - x_j)$ .

Figure 1 shows the formation configuration for two UGV. The transformation between  $F_{ij}$  and  $\bar{F}_{ij}$  is straightforward.

The formation error for robot-pair  $i$  and  $j$  is then defined as  $e_{ij} = \bar{F}_{ij}^d - \bar{F}_{ij}$ .

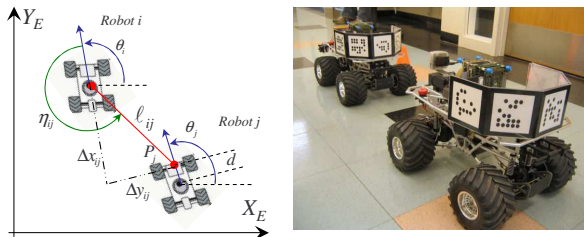


Fig. 1. Formation configuration for two UGV.

#### A. MPC/Dual-Mode MPC

Different from conventional control which uses pre-computed control laws, MPC is a technique in which the current control action is obtained by solving, at each sampling instance, a finite-horizon optimal control problem. Each optimization yields an open-loop optimal control sequence

and the first control of this sequence is applied to the plant until the next sampling instance.

Control (tracking, stabilizing) of robots with nonholonomic constraints can be handled with same MPC algorithm. See the tracking-stabilizing-tracking simulation below.

Let us define the formation error for the  $j^{\text{th}}$  robot in a robot-pair  $(R_i, R_j)$

$$x_j^e = \begin{bmatrix} \Delta x_{ij}^d - \Delta x_{ij} \\ \Delta y_{ij}^d - \Delta y_{ij} \\ \theta_i - \theta_j \end{bmatrix}. \quad (3)$$

To obtain the current control  $u_j(k)$  at time  $t_k$ , where  $k$  is a nonnegative integer ( $k \in \mathbb{Z}^*$ ), a finite-horizon optimal control problem

$$P(x_j^e, k) := \min_{u_j} \{J_H(x_j^e, k, u_j)\},$$

must be solved online. The performance index  $J_H(x_j^e, k, u_j)$  is defined as

$$\sum_{m=1}^H \|x_j^e(k+m; x_j^e, k)\|_Q^2 + \sum_{m=1}^H \|u_j(k+m-1)\|_R^2.$$

$H \in \mathbb{N}$  is the horizon length (for simplicity, the prediction horizon equals the control horizon in this paper).  $Q$  and  $R$  are positive definite symmetric matrices.

To ensure stability of the MPC algorithm, a terminal equality constraint  $x_j^e(k+H) = 0$  is commonly used. Therefore,  $\Delta x_{ij} \rightarrow \Delta x_{ij}^d$ ,  $\Delta y_{ij} \rightarrow \Delta y_{ij}^d$  and  $\theta_j \rightarrow \theta_i$ . However, an equality constraint usually makes the optimal control problem hard to solve. To balance the stability and feasibility, the terminal equality constraint can be relaxed to a terminal region. The MPC algorithm is only required to drive the error system to the edge of the terminal region. Inside the terminal region, a stabilizing terminal controller is switched in and it drives the error system to the equilibrium point. Such MPC algorithm is dual-mode [14].

For a robot-pair  $(R_i, R_j)$ , which has an ordered pair  $(V_i, V_j) \in \mathcal{E}$  in the *formation control graph*  $\mathcal{G}$  and a *set point*  $F_{ij}^d \in \mathcal{F}$ , a control input  $u_j$  needs to be determined for robot  $j$ . With the assumption that robot  $i$ 's current and future control action  $\hat{u}_i$  are known to robot  $j$ , the formation-error system for robot  $j \in \{1, \dots, N\}$  at time  $t_k$  can be defined as follows

$$\begin{aligned} x_j^e(k+1) &= f(x_j^e(k), u_j(k)), \\ x_j^e(k) &\in \mathcal{X}, u_j(k) \in \mathcal{U}, \end{aligned} \quad (4)$$

where  $f(\cdot)$  is continuous at the origin, with  $f(0,0) = 0$ ;  $\mathcal{X} \subset \mathbb{R}^3$  contains the origin in its interior;  $\mathcal{U}$  is a compact subset of  $\mathbb{R}^2$  containing the origin in its interior.

Now let us define the terminal region  $\mathcal{X}_f$ , which is a convex compact subset of  $\mathcal{X}$  containing the origin in its interior. Therefore, we can define a set  $\mathcal{X}_f^c$ , where  $\mathcal{X}_f^c \cup \mathcal{X}_f = \mathcal{X}$  and  $\mathcal{X}_f^c \cap \mathcal{X}_f = \emptyset$ . Inside  $\mathcal{X}_f$ , a stabilizing terminal controller  $u_j^T$  is employed to drive the system (4) back to the origin. Note, the terminal region  $\mathcal{X}_f$  should be positively invariant for the system  $x_j^e(k+1) = f(x_j^e(k), u_j^T(k))$ . Methods for constructing  $\mathcal{X}_f$ , which indeed is the terminal

controller's region of attraction, can be found in [14], [18] (local linear controller case). For a nonlinear controller which has a region of attraction  $\mathcal{X}$ , such as (12), the terminal region can be a ball  $B_r$ , which contains the origin.

The incremental cost in the optimal control problem for robot  $j \in \{1, \dots, N\}$  is defined in the manner of [18]

$$L(x_j^e, u_j) = \lambda(x_j^e) \mathcal{L}(x_j^e, u_j), \quad (5)$$

where

$$\lambda(x_j^e) = \begin{cases} 0, & \text{if } x_j^e \in \mathcal{X}_f \\ 1, & \text{otherwise} \end{cases},$$

and

$$\mathcal{L}(x_j^e, u_j) = \|x_j^e\|_Q^2 + \|u_j\|_R^2. \quad (6)$$

Clearly, the incremental cost  $L(\cdot)$  is continuous at the origin, with  $L(0, 0) = 0$ .

For robot  $j \in \{1, \dots, N\}$ , given  $(V_i, V_j) \in \mathcal{E}$  and  $F_{ij}^d \in \mathcal{F}$ ,  $q_i(k)$  and  $q_j(k)$ ,  $u_i(k+H-1, \dots, k; k)$  at any update time instance  $t_k$ , the optimal control problem is now defined

$$P(x_j^e, k) := \min_{u_j} \{J_H(x_j^e, k, u_j)\}, \quad (7)$$

where

$$J_H(x_j^e, k, u_j) = \sum_{m=1}^H L(x_j^e(k+m; k), u_j(k+m-1; k)), \quad (8)$$

subject to

$$\begin{aligned} x_j^e(k+1) &= f(x_j^e(k), u_j(k)), \\ x_j^e(k+H) &\in \mathcal{X}_f, u_j(k) \in \mathcal{U}. \end{aligned} \quad (9)$$

From the definition of incremental cost, the objective function  $J_H(x_j^e, k, u_j)$  is greater than or equal to 0 and  $J_H(x_j^e, k, u_j) = 0$  only when  $x_j^e = 0$  and  $u_j = 0$ .

The solution of optimal control problem (7) is denoted as  $u^*(k) = u_j^*(k+m-1; k)$ . The optimal state trajectory under this control action is  $x_j^{e*}(k) = x_j^{e*}(k+m; k)$ . The corresponding optimal performance index is  $J_H^*(k) = J_H(x_j^{e*}(k+m; k), k, u_j^*(k+m-1; k))$  where  $m \in [1, \dots, H]$ .

Now the dual-mode model predictive controller for robot  $j \in \{1, \dots, N\}$  is stated in the following algorithm.

**Algorithm:**

**Data:** initial states of robots  $q_i(0)$ ,  $q_j(0)$ ,  $H \in \mathbb{N}$ .

**Initial:** At time instance  $t_k = 0$ , if  $x_j^e(0) \in \mathcal{X}_f$ , switch to the terminal controller  $u_j^T$  for all  $k$  such that  $x_j^e(k) \in \mathcal{X}_f$ . Else set  $\hat{u}_i(l; k) = 0$  and  $\hat{u}_j(l; k) = 0$  for all  $l \in [k, \dots, k+H-1]$ . Then solve optimal control problem (7) for robot  $j$  and obtain  $u_j^*(l; k)$ , where  $l \in [k, \dots, k+H-1]$ . Set  $u_j^o(k) = u_j^*(k; k)$  and apply  $u_j^o(k)$  to the system.

**Controller:**

- 1) At any time instance  $t_k$ :
  - a) Measure current state  $q_j(k)$  and measure or receive current state  $q_i(k)$ .
  - b) If  $x_j^e(k) \in \mathcal{X}_f$ , switch to the terminal controller  $u_j^T$  for all  $k$  such that  $x_j^e(k) \in \mathcal{X}_f$ . Set  $u_k^o(k) = u_j^T(k)$ .

- c) Else, with  $\hat{u}_i(l; k)$  and  $\hat{u}_j(l; k)$  as initial guess, solve optimal control problem (7) for robot  $j$  and obtain  $u_j^*(l; k)$ , where  $l \in [k, \dots, k+H-1]$ . Set  $u_j^o(k) = u_j^*(k; k)$ .

2) Over time interval  $[t_k, t_{k+1})$ :

- a) Apply  $u_j^o(k)$  to the system.
- b) If  $x_j^e(k) \in \mathcal{X}_f$ , set  $\hat{u}_j(l; k+1) = u_j^T(l)$ ,  $l \in [k+1, \dots, k+H]$ .
- c) Else, compute  $\hat{u}_j(l; k+1)$  as
$$\begin{cases} u_j^*(l; k) & l \in [k+1, \dots, k+H-1] \\ u_j^T(k+H) & l = k+H \end{cases}$$
- d) Transmit  $\hat{u}_j(\cdot; k+1)$  to all robot  $n$  that  $(v_j, v_n) \in \mathcal{E}$  and receive  $\hat{u}_i(\cdot; k+1)$ .

**B. Input-Output Feedback Linearization Controller**

For the choice of terminal controller, an input-output feedback linearization controller (denoted as Separation Bearing Controller, SBC) developed in [17] can be used. *Set points*, are desired distance  $l_{ij}^d$  and desired orientation  $\eta_{ij}^d$  relative to the leader. The control law determining  $u_j = [v_j \ \omega_j]^T$  based on the position of  $R_i$ , which stabilizes the position of  $R_j$  relative to  $R_i$ , is [17]

$$\begin{aligned} v_j &= s_{ij} \cos \gamma_{ij} - l_{ij}(b_{ij} + \omega_i) \sin \gamma_{ij} + v_i \cos(\theta_i - \theta_j), \\ \omega_j &= \frac{1}{d} (s_{ij} \sin \gamma_{ij} + l_{ij}(b_{ij} + \omega_i) \cos \gamma_{ij} \\ &\quad + v_i \sin(\theta_i - \theta_j)), \end{aligned} \quad (10)$$

where

$$\begin{aligned} \gamma_{ij} &= \eta_{ij} + \theta_i - \theta_j, \\ s_{ij} &= k_1(l_{ij}^d - l_{ij}), \\ b_{ij} &= k_2(\eta_{ij}^d - \eta_{ij}), \end{aligned} \quad (11)$$

and  $k_1$  and  $k_2$  are positive constants.

**C. Robust Formation Controller**

Notice that, the SBC controller requires leader's velocity information, which may not be available. To overcome this limitation, a robust control law,  $u_j^R$ , which stabilizes the formation between robot-pair  $i$  and  $j$  is proposed in [13]

$$\begin{aligned} u_j^R &= g^{-1}(\cdot) \left( \begin{bmatrix} \frac{1}{l_{ij}} \sin^2 \gamma_{ij} \\ \frac{1}{l_{ij}^2} \cos \gamma_{ij} \sin \gamma_{ij} \end{bmatrix} v_j^2 \right. \\ &\quad \left. - 2K e_{ij} - K^2 e_{ij} - \beta_1 \operatorname{sgn}(e_{ij}) \right), \end{aligned} \quad (12)$$

where

$$g(\cdot) = \begin{bmatrix} -\cos \gamma_{ij} & -v_j \sin \gamma_{ij} \\ \frac{1}{l_{ij}} \sin \gamma_{ij} & -\frac{v_j}{l_{ij}} \cos \gamma_{ij} \end{bmatrix} \in \mathbb{R}^{2 \times 2},$$

$v_j$  is the linear velocity of robot  $j$ ,  $K = \begin{bmatrix} k_1 & 0 \\ 0 & k_2 \end{bmatrix}$ ,  $k_{1,2} \in \mathbb{R}_+$ , and  $\beta_1$  are positive constant control gains. Details of this robust formation controller will be explained in Section IV.

IV. STABILITY RESULTS

A. Dual-Mode MPC

Since inside  $\mathcal{X}_f$ , a stabilizing terminal controller  $u_j^T$  is used, when the state enters  $\mathcal{X}_f$ , the error system will converge to the origin according to the stability properties of controller  $u_j^T$ . The stability of the system (4) is guaranteed if the state,  $x_j^e(k)$ , starting from any  $x_j^e(0) \in \mathcal{X} \setminus \mathcal{X}_f$ , reaches  $\mathcal{X}_f$  within finite time under the the dual-mode MPC Algorithm (see Fig. 2).

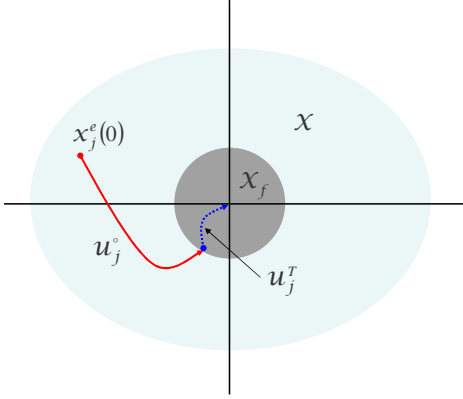


Fig. 2. State trajectory.

**Assumption 4.1:** For the incremental cost  $L(x_j^e, u_j)$ , there exists a  $\mathcal{K}$ -function  $\kappa(\cdot)$  such that  $L(x_j^e, u_j) \geq \kappa(\|x_j^e\|)$  for all  $x_j^e \in \mathcal{X} \setminus \mathcal{X}_f$  and all  $u_j \in \mathcal{U}$ .

**Assumption 4.2:** For all  $x_j^e(k) \in \mathcal{X} \setminus \mathcal{X}_f$ ,  $u^*(k)$  exists and is unique.

Before presenting the main result of this sub-section, we state the following lemma (motivated by [14], [18]) which will be invoked later.

**Lemma 4.3:** Suppose assumptions 4.1, 4.2 are satisfied. Then for all  $k \in \mathbb{Z}^*$  such that both  $x_j^e(k)$  and  $x_j^e(k+1)$  are in  $\mathcal{X} \setminus \mathcal{X}_f$ , under the dual-mode MPC algorithm, the following inequality

$$J_H^*(k+1) - J_H^*(k) \leq -\kappa(\|x_j^e(k+1)\|) \quad (13)$$

holds.

**Proof:** By Assumption 4.2,  $u_j^*(k)$  and  $u_j^*(k+1)$  exist, so do the optimal performance index  $J_H^*(k)$  and  $J_H^*(k+1)$ .

To find  $J_H^*(k+1)$ , the dual-mode MPC algorithm solves the optimal control problem (7) from an initial control guess  $\hat{u}_j(l; k+1)$ ,  $l \in [k+1, \dots, k+H]$ , which is constructed from the result of previous optimization on time  $t_k$ . Obviously,  $J_H^*(k+1) \leq \hat{J}_H(x_j^e(\cdot), k+1, \hat{u}_j(l; k+1))$ . Therefore,

$$J_H^*(k+1) - J_H^*(k) \leq \hat{J}_H(x_j^e(\cdot), k+1, \hat{u}_j(l; k+1)) - J_H^*(k). \quad (14)$$

Follow the construction of  $\hat{u}_j(l; k+1)$ , which is described in the algorithm given in Section III-A, we have

$$\begin{aligned} & \hat{J}_H(x_j^e(\cdot), k+1, \hat{u}_j(l; k+1)) - J_H^*(k) = \\ & -L(x_j^{e*}(k+1; k), u_j^*(k; k)) \\ & +L(x_j^e(k+H+1; k), u_j^T(k+H)). \end{aligned} \quad (15)$$

Since  $x_j^e(k+H+1; k) \in \mathcal{X}_f$ , we have

$$L(x_j^e(k+H+1; k), u_j^T(k+H)) = 0.$$

In addition, assuming the system model is perfect, we have

$$L(x_j^{e*}(k+1; k), u_j^*(k; k)) = L(x_j^e(k+1), u_j^*(k; k)).$$

Therefore,

$$J_H^*(k+1) - J_H^*(k) \leq -L(x_j^e(k+1), u_j^*(k; k)). \quad (16)$$

Clearly, with Assumption 4.1, inequality (13) holds. ■

We now state the main stability result for the proposed dual-mode MPC in the following theorem.

**Theorem 4.4:** Let assumptions 4.1 and 4.2 be satisfied. Using the terminal controller (12) and the kinematic model (1), the dual-mode MPC is asymptotically stabilizing with a region of attraction  $\mathcal{X}$ .

**Proof:** According to the analysis at the beginning of this section, since inside  $\mathcal{X}_f$ , a stabilizing terminal controller  $u_j^T$  is used, when the state enters  $\mathcal{X}_f$ , the error system will converge to the origin asymptotically. We only need to prove that from any  $x_j^e(0) \in \mathcal{X} \setminus \mathcal{X}_f$ , under the dual-mode model predictive controller, the state will be driven into  $\mathcal{X}_f$  within finite time.

As the definition of  $\mathcal{X}_f$ , it contains the origin in its interior. There must exist a constant  $r > 0$  such that for all  $x_j^e(\cdot) \in \mathcal{X} \setminus \mathcal{X}_f$ , we have  $\|x_j^e(\cdot)\| \geq r$ . Then, with the definition of  $\mathcal{K}$ -function, inequality

$$\kappa(\|x_j^e(\cdot)\|) \geq \kappa(r) \quad (17)$$

holds.

Suppose that a finite time  $t_k$  doesn't exist such that  $x_j^e(k) \in \mathcal{X}_f$ . Because of Lemma 4.3, by adding inequality (13) from 0 to  $k$ , we have

$$\begin{aligned} J_H^*(k) - J_H^*(0) & \leq -\sum_{n=0}^k \kappa(\|x_j^e(n)\|) \\ & \leq -k \min\{\kappa(\|x_j^e(0)\|), \dots, \kappa(\|x_j^e(k)\|)\}, \end{aligned} \quad (18)$$

for all  $k \in \mathbb{Z}^*$ . Then according to inequality (17), we have

$$-k \min\{\kappa(\|x_j^e(0)\|), \dots, \kappa(\|x_j^e(k)\|)\} \leq -k\kappa(r). \quad (19)$$

This means

$$J_H^*(k) - J_H^*(0) \leq -k\kappa(r), \quad \text{for all } k \in \mathbb{Z}^*. \quad (20)$$

However, (20) implies that  $J_H^*(k) \rightarrow -\infty$  as  $k \rightarrow \infty$ . This contradicts that  $J_H(k) \geq 0$  for all  $k \in \mathbb{Z}^*$ . Therefore, there exists a time  $t_k$  such that  $x_j^e(k) \in \mathcal{X}_f$ . The stabilizing property of the controller follows. ■

B. Input-Output Feedback Linearization Controller

**Theorem 4.5:** Assume that the lead vehicle's linear velocity along the path  $g(t) \in SE(2)$  is lower bounded i.e.,  $v_i \geq V_{\min} > 0$ , its angular velocity is also bounded i.e.,  $\|\omega_i\| < W_{\max}$ , the relative velocity  $\delta_v \equiv v_i - v_j$  and relative orientation  $\delta_\theta \equiv \theta_i - \theta_j$  are bounded by small positive numbers  $\varepsilon_1, \varepsilon_2$ , and the initial relative orientations  $\|\theta_i(t_0) - \theta_j(t_0)\| < c_1\pi$ , with  $0 < c_1 < 1$ . If the control

law (10) is applied to robot  $R_j$ , then the formation is stable, and the system outputs  $l_{ij}, \eta_{ij}$  converge exponentially to the desired values [19].

**Remark 4.6:** Note that, to guarantee stable behavior of  $R_j$ , we would require  $v_i > 0$ . Otherwise, the internal dynamics  $\theta_j$  of  $R_j$  may be unstable. Let the orientation error be expressed as  $\dot{e}_\theta = \omega_i - \omega_j$ . After incorporating the angular velocity for the follower (10), we obtain

$$\dot{e}_\theta = -\frac{v_i}{d_j} \sin e_\theta + \xi(\omega_i, e_\theta), \quad (21)$$

where  $\xi(\cdot)$  is a nonvanishing perturbation for the nominal system (equation (21) with  $\xi(\cdot) = 0$ ), which is itself (locally) exponentially stable. By using the stability of perturbed systems, it can be shown that system (21) is stable when  $v_i > 0$ . A detailed proof of Theorem 4.5 and explanation of internal dynamics can be found in [19].

### C. Robust Formation Controller

Let us define the following filtered signal  $r(t) = [r_1 r_2]^T \in \mathbb{R}^2$

$$r(t) = \dot{e}_{ij} + K e_{ij}. \quad (22)$$

Differentiating (22) with respect to time, we can get

$$\begin{aligned} \dot{r}(t) = & - \left[ \begin{array}{c} \frac{1}{l_{ij}} \sin^2 \gamma_{ij} \\ \frac{1}{l_{ij}^2} \cos \gamma_{ij} \sin \gamma_{ij} \end{array} \right] v_j^2 + g(\cdot) u_j + f_1(\cdot) \varpi_i \\ & + f_2(\cdot) \dot{\varpi}_j + f_3(\cdot) \varpi_i v_i + K \dot{e}_{ij}. \end{aligned} \quad (23)$$

where  $f_1(\cdot), f_2(\cdot)$ , and  $f_3(\cdot)$  are functions of  $F_{ij}(t), v_j(t)$ , and  $\gamma_{ij}(t)$ .

**Assumption 4.7:** Inside the formation, the leader robot is stably tracking some desired trajectories  $\varpi_i^d = [v_i^d \omega_i^d]^T$ ,  $\dot{\varpi}_i^d = [\dot{v}_i^d \dot{\omega}_i^d]^T \in \mathbb{R}^2$  with  $\varpi_i^d, \dot{\varpi}_i^d, \ddot{\varpi}_i^d \in \mathcal{L}_\infty$  so that we can assume  $\varpi_i, \dot{\varpi}_i, \ddot{\varpi}_i \in \mathcal{L}_\infty$ .

**Assumption 4.8:** All other terms in (23) except  $\varpi_i$  and  $\dot{\varpi}_i$  are known.

**Lemma 4.9:** Let the auxiliary function  $\Gamma(t) \in \mathbb{R}$  be defined as follows

$$\Gamma \triangleq r^T [f_1(\cdot) \varpi_i + f_2(\cdot) \dot{\varpi}_i + f_3(\cdot) \varpi_i v_i - \beta_1 \text{sgn}(e_{ij})]. \quad (24)$$

If the control gain  $\beta_1$  is selected to satisfy the sufficient condition

$$\beta_1 > \frac{\|f_1(\cdot) \varpi_i + f_2(\cdot) \dot{\varpi}_i + f_3(\cdot) \varpi_i v_i\|_2 + k_{min}^{-1} \left\| \frac{d(f_1(\cdot) \varpi_i + f_2(\cdot) \dot{\varpi}_i + f_3(\cdot) \varpi_i v_i)}{dt} \right\|_2}{}, \quad (25)$$

where  $k_{min} = \min \{k_1, k_2\}$ , then

$$\int_{t_0}^t \Gamma(\tau) d\tau \leq \zeta_b, \quad (26)$$

where the positive constant  $\zeta_b \in \mathbb{R}$  is defined as

$$\zeta_b \triangleq \beta_1 \|e_{ij}(t_0)\|_1 - e_{ij}^T(t_0) [f_1(t_0) \varpi_i(t_0) + f_2(t_0) \dot{\varpi}_i(t_0) + f_3(t_0) \varpi_i(t_0) v_i(t_0)], \quad (27)$$

where the notation  $\|\cdot\|_1$  denotes the  $\mathcal{L}_1$  norm.

**Theorem 4.10:** The control law of (12) ensures that all system signals are bounded under closed-loop operation and the tracking error is asymptotically stable in the sense that  $\lim_{t \rightarrow \infty} e_{ij}(t), \dot{e}_{ij}(t) = 0$ .

**Remark 4.11:** Notice that, the robust controller proposed here does not require the leader robot's velocity information and there are no internal dynamics. This is a big improvement to the SBC controller described in Section III-B. The only limitation here is that the reference robot's velocity can't be zero. Otherwise,  $v_j$  needs to be zero and the inverse of  $g(\cdot)$  cannot be computed. In summary, for the SBC controller, it fails when  $v_i \leq 0$ . For the robust controller, it only fails when  $v_i = 0$ . In addition, this robust controller is globally stable, which means that it has a region of attraction  $\mathcal{X}$ . This alleviates the difficulty of finding a terminal region.

## V. SIMULATION RESULTS

The effectiveness of the control algorithms presented in Section III is investigated by numerical simulations. In the figures, each robot is depicted by an arrow within a circle. The orientation of the robot is shown by the orientation of the arrow.

### A. Tracking-Stabilizing-Tracking

A realistic scenario is illustrated in Figure 3. The reference robot 1 first moves forward from position (0, 0). Then it stops for some time and finally starts to move backward. This scenario happens when some algorithms are implemented for the reference robot 1 to avoid obstacles. Usually this tracking-stabilizing-tracking case is not considered under a single controller approach. To keep the formation, a controller switching is required. However, a simulation shows that this case can be handled within the MPC framework. The desired formation is  $F_{12}^d = [-20, -10]$  and it is achieved by the MPC controller. Note, a conventional MPC controller is used here.

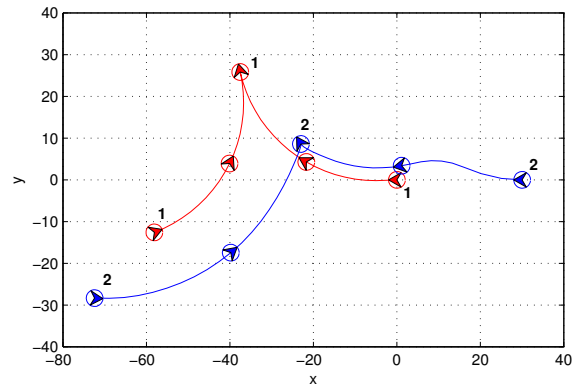


Fig. 3. Trajectory of a robot following a reference vehicle which moves forward, stops, and then moves backward according to an MPC controller.

### B. Follow a Leader Moving Backward

Figure 4 shows the response of robot  $j$  following a reference robot  $i$  which is moving backward under the robust

formation controller (12). This scenario cannot be handled by the SBC controller since it fails when the leader's velocity is negative. The desired formation is  $\bar{F}_{ij}^d = [100, \frac{5\pi}{4}]$ . Robot  $i$  starts from position  $(0, 0)$  and moves backward with constant speed  $v_i = -17.5$ . Robot  $j$  starts from  $(150, 200)$  and moves backward. The formation is achieved by the robust formation controller.

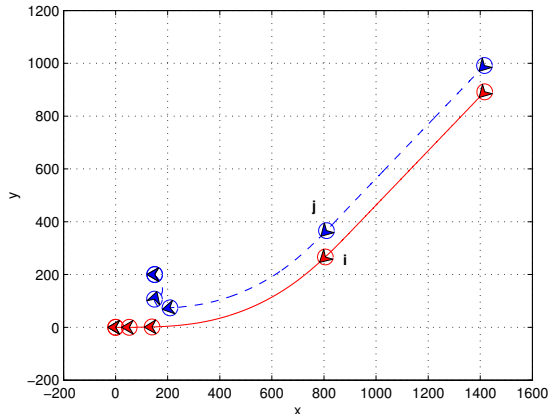


Fig. 4. Trajectory of a robot following a reference robot which is moving backward according to the robust formation controller.

### C. Control of a Chain of robots

The formation response shown in Figure 5 is according to a dual-mode MPC with the robust formation controller (12) as the terminal controller. The prediction horizon is set to  $H = 6$ . The formations for each robot-pair are  $F_{12}^d = F_{23}^d = F_{34}^d = F_{45}^d = [-20 \ 0]^T$ . The control constrain set is defined as  $\mathcal{U} = \{[V \ \omega]^T \in \mathbb{R}^2 : 15 \leq V \leq 50, -0.3 \leq \omega \leq 0.3\}$ .

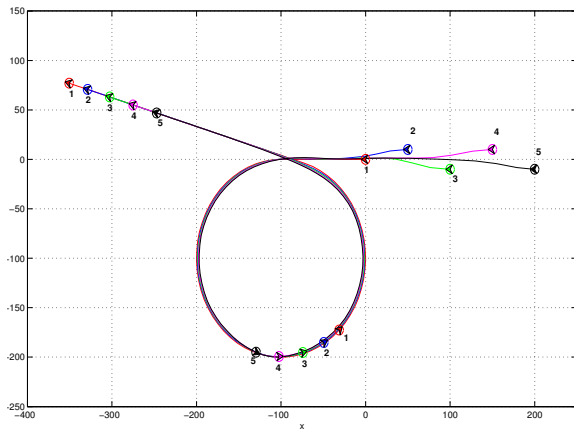


Fig. 5. Five robots in chain formation according to a dual-mode MPC with robust formation controller as the terminal controller.

## VI. CONCLUSIONS

In this paper, a dual-mode MPC algorithm that allows a team of mobile robots to navigate in formations is developed and proven to be stable. Simulations show the effectiveness

of the proposed dual-mode MPC algorithm. Additionally, we show that it is more convenient to put the tracking and point stabilizing problems of nonholonomic robots inside the MPC framework. For the choice of stabilizing terminal controller, analysis and simulation show that the robust formation controller is better than the SBC controller.

### ACKNOWLEDGEMENTS

This work is supported in part by NSF grant CAREER #0348637 and by the U.S. Army Research Office under grant DAAD19-03-1-0142 (through the University of Oklahoma).

### REFERENCES

- [1] R. Vidal, O. Shakernia, and S. Sastry, "Formation control of nonholonomic mobile robots with omnidirectional visual servoing and motion segmentation," in *Proc. IEEE Int. Conf. Robot. Automat.*, vol. 1, Sept. 2003, pp. 584–589.
- [2] W. B. Dunbar and R. M. Murray, "Distributed receding horizon control for multi-vehicle formation stabilization," *Automatica*, vol. 2, no. 4, pp. 549–558, 2006.
- [3] F. Borrelli, T. Keviczky, K. Fregene, and G. J. Balas, "Decentralized receding horizon control of cooperative vehicle formations," in *Proc. IEEE Conf. on Decision and Control*, Seville, Spain, December 2005, pp. 3955–3960.
- [4] R. W. Brockett, "Asymptotic stability and feedback stabilization," in *Differential Geometric Control Theory*, R. W. Brockett, R. S. Millman, and H. J. Sussmann, Eds., Birkhuser, Boston, MA, 1983, pp. 181–191.
- [5] H. G. Tanner and K. J. Kyriakopoulos, "Discontinuous backstepping for stabilization of nonholonomic mobile robots," in *Proc. IEEE Int. Conf. Robot. Automat.*, 2002, pp. 3948–3953.
- [6] R. Murray and S. Sastry, "Nonholonomic motion planning—steering using sinusoids," *IEEE Trans. on Automatic Control*, vol. 38, no. 5, pp. 700–716, May 1993.
- [7] W. E. Dixon, D. M. Dawson, E. Zergeroglu, and A. Behal, *Nonlinear control of wheeled mobile robots*. Secaucus, NJ: Springer, 2001.
- [8] A. N. Venkat, J. B. Rawlings, and S. J. Wright, "Stability and optimality of distributed model predictive control," in *Proc. IEEE Conf. on Decision and Control*, Seville, Spain, December 2005, pp. 6680–6685.
- [9] M. Morari and J. H. Lee, "Model predictive control: past, present and future," *Computers and Chemical Engineering*, vol. 23, pp. 667–682, 1999.
- [10] D. Gu and H. Hu, "A stabilizing receding horizon regulator for nonholonomic mobile robots," *IEEE Trans. Robot. Automat.*, vol. 21, no. 5, pp. 1022–1028, October 2005.
- [11] —, "Receding horizon tracking control of wheeled mobile robots," *IEEE Trans. Contr. Syst. Technol.*, vol. 14, no. 4, pp. 743–749, July 2006.
- [12] K. Wesselowski and R. Fierro, "A dual-mode model predictive controller for robot formations," in *Proc. IEEE Conf. on Decision and Control*, December 2003, pp. 3615–3620.
- [13] F. Xie, X. Zhang, R. Fierro, and M. Motter, "Autopilot-based nonlinear uav formation controller with extremum-seeking," in *Proc. IEEE Conf. on Decision and Control*, December 2005, pp. 4933–4938.
- [14] H. Michalska and D. Q. Mayne, "Robust receding horizon control of constrained nonlinear systems," *IEEE Trans. Automat. Contr.*, vol. 38, no. 11, pp. 1623–1633, November 1993.
- [15] H. Tanner, G. Pappas, and V. Kumar, "Leader-to-formation stability," *IEEE Trans. Robot. Automat.*, vol. 20, pp. 443–455, 2004.
- [16] O. A. Orqueda and R. Fierro, "Vision-based nonlinear decentralized controller for unmanned vehicles," in *Proc. IEEE Int. Conf. Robot. Automat.*, May 2006, pp. 1–6.
- [17] J. Desai, J. P. Ostrowski, and V. Kumar, "Controlling formations of multiple mobile robots," in *Proc. IEEE Int. Conf. Robot. Automat.*, Leuven, Belgium, May 1998, pp. 2864–2869.
- [18] P. O. M. Scokaert, D. Q. Mayne, and J. B. Rawlings, "Suboptimal model predictive control (feasibility implies stability)," *IEEE Trans. Automat. Contr.*, vol. 44, no. 3, pp. 648–654, March 1999.
- [19] R. Fierro, P. Song, A. K. Das, and V. Kumar, "Cooperative control of robot formations," in *Cooperative Control and Optimization*, ser. Applied Optimization, R. Murphey and P. Pardalos, Eds. Dordrecht: Kluwer Academic Press, 2002, vol. 66, ch. 5, pp. 73–93.